PLASTIC BUCKLING OF OPEN SHELLS UNDER IMPACT LOADS

Sérgio Seiji Teramoto
Group of Solid Mechanics and Structural Impact
Departament of Mechatronics and Mechanical Systems Engineering
University of São Paulo
sergio.teramoto@poli.usp.br

Marcílio Alves
Group of Solid Mechanics and Structural Impact
Departament of Mechatronics and Mechanical Systems Engineering
University of São Paulo
maralves@usp.br

Abstract. This paper presents experimental data on the transition between global and progressive buckling of open channels subjected to axial impact loads. The experiments were used to assist in the numerical simulation of this phenomenon, which found that buckling transition cannot be clearly characterised for these open shells by considering only the overall final buckling shape. Influence of geometry, boundary conditions and inertia effects on the final deformed configuration is also explored and discussed. An extended version of this article was presented in the 8th International Symposium on Plasticity and Impact Mechanics, New Delhi, India, 2003

Keywords.: buckling, impact, open shells

1. Introduction

The axial crushing of shell like structures is one of the most used mechanisms to absorb impact energy, leading to important applications in the design of crashworthy structures. The axisymmetric collapse mode of the aluminium circular tube in Fig. 1(a) is clearly progressive, i.e. a new fold is formed after a previous one is completed. Usually, an axisymmetric collapse absorbs more energy per wrinkle than the non-axisymmetric buckling mode in Fig. 1(b). Further, much less energy is necessary to buckle the same length aluminium tube of Fig. 1(a) but now collapsing according to Fig. 1(c). This global buckling mode is characterized by a few wrinkles, usually in the middle and at the ends.

The various buckling patterns shown in Fig. 1 were obtained for the same boundary condition but with different axial impact mass and velocity. It has been shown (Alves and Karagiozova, 2002; Alves and Karagiozova, 2001) that, generally speaking, the higher the impact velocity the more stable the shell response, leading to a progressive buckling mode.

A literature review on plastic buckling of shells (Alghamdi, 2001) shows that the axisymmetric mode of collapse of a shell under axial load was first analysed by Alexander (Alexander, 1969). Wierzbicki and Abramowicz (1983), developed an element whose folding mode allowed the estimation of the mean collapse load of box columns. Abramowicz and Jones (1986), have improved the modelling of square tubes using these elements but considering a more accurate effective crushing distance. Chen and Wierzbicky (2001), investigated

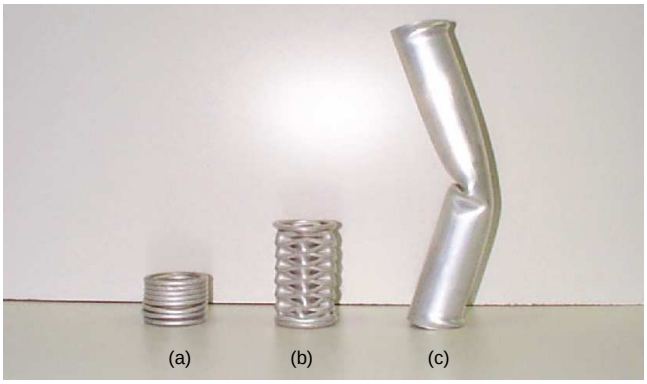

Figure 1: Basic collapse modes of a cylindrical shell under axial impact mass: (a) axisymmetric folding, (b) diamond folding, (c) global buckling.

the merits of different shell cross-section profile in absorbing more or less energy and they concluded that there is no improvement on the specific energy absorption, SEA, if a single or double internal wall is used. The SEA can improve by up to 300% if the columns were filled with a foam and optimized dimensions for shell geometry and foam density were used. White *et al.* (White et al., 1999; White and Jones, 1999) investigated the collapse behaviour of top hat and double hat cross-sections, greatly affected by the flange width. Karagiozova *et al.* (2000), shows the influence of the impact velocity and mass on the collapse of shells and the major parameters which could trigger either progressive or dynamic buckling in cylindrical shells were analysed. Lu and Mao (2001), performed an analysis of the plastic buckling of shells, focusing on the critical loads and mode shapes, which allowed the investigation of the influence of the shell geometry in triggering a particular buckling mode shape.

Various modes of collapse of thin-walled tubes were experimentally investigated by Andrews *et al.* (1983), and, more recently, by Guillow *et al.* (2001) . Also, Abramowicz and Jones (1997) present extensive experimental data exploring the transition between global bending and progressive buckling of circular and square tubes. They found that the transition to Euler mode of collapse is given by a simple geometrical relation, so not capturing the decisive influence of the impact velocity on triggering one or other mode of collapse, as found in Alves *et al.* (2001) . Recently, Jensen *et al.* (2001) investigated in a pure numerical way the transition from progressive to global buckling of square aluminium tubes, in contrast with Hsu and Jones (2001) , who approached the same subject from an experimental point of view using circular and square stainless steel tubes.

There is an important lack of understanding on the factors which mark the threshold between a global and a progressive collapse. Abramowicz and Jones (1997) , and Mahmood and Paluszny (1982) suggested analytical models for this phenomenon, motivating the approach undertaken by Karagiozova and Alves (2002) for buckling transition of cylindrical shells. Complementary to this later study, it is here pursued a numerical investigation of the global to progressive transition phenomenon found in open shells resembling a ⊏ shape in view of better designing them to absorb impact energy in a possible collision.

2. Experimental procedure

Some previous experimental observations on the buckling transition of circular shells subjected to axial impact (Karagiozova and Alves, 2002; Alves and Karagiozova, 2001) have shown that the higher the impact velocity the more stable the shell is. Using this very same finding for circular shells, it is here explored the influence of the impact velocity in determining the collapse mode of open shells.

2.1. Material characterization

Tensile specimens were prepared and cut in the roll direction from the aluminium 1.5mm thick sheets used to manufacture the shells. Tests were performed in a standard tensile test machine using axial electronic extensometers. The load-displacement curve was recorded and procedures similar to the ones described in Alves and Jones (2002), were used to plot the true stress–strain curve in Fig. 2(a).

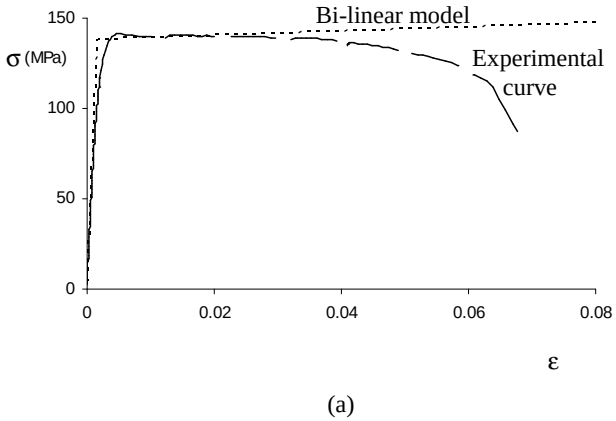

(a)

σ_y (MPa)	138
E (MPa)	76666.7
E_h (MPa)	123.3
ε_r	0.08

(b)

Figure 2: (a) True stress–strain curve for the aluminium alloy. (b) Main mechanical material properties obtained from a bilinear interpolation of a quasi-static test.

It is evident from Fig. 2(a) that the material in play has a low strain hardening modulus and it has a relatively low ductility. To define a bi-linear elastic-plastic material model one needs to extrapolate the measured curve in the plastic regime with a straight line from a given flow stress. The inclination of this line, which represents E_h for a unity strain, and the flow stress are not easily defined in the curve, so some

tensile tests were performed on specimens made of the same aluminium alloy but with a lateral notch. The load–displacement curve was measured and a finite element simulation was run using the software ABAQUS. Various run were executed with different flow stress and plastic modulus until the numerical load–displacement curve matched the experimental data. As a result, a bi-linear elastic-plastic material model was adopted with the parameters indicated in Fig. 2(b). It is assumed here that the aluminium alloy has a negligible sensitivity to the strain rate, so that the quasi-static curve in Fig. 2(a) was used in all the simulations.

2.2. Quasi-static and impact tests

Aluminium open cross-section profiles, Fig. 3, with $A/B = 1$, 2 and 3, denominated specimens A, B and C, respectively, having lengths of 250mm and 500mm, were tested on the drop hammer described in Alves and Birch (1999), and shown in Fig. 4, with a varying impact mass from $G = 22$kg to $G = 118$kg.

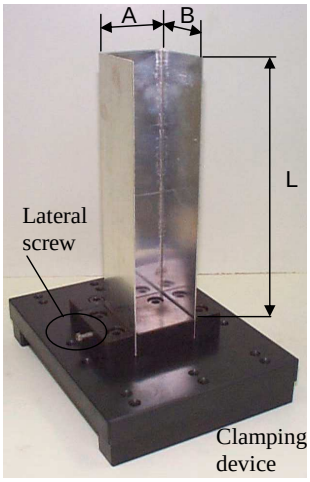

Specimen	L (mm)	A (mm)	B (mm)
A250	250	68	68
A500	500	68	68
B250	250	102	51
B500	500	102	51
C250	250	122	41
C500	500	122	41

Figure 3: Dimensions of the open shells and details of the clamping device.

Figure 4: Drop hammer for impact tests

Some experimental results are shown in Fig. 5 and 6, which describes, in the caption, the geometry and test variables. Boundary conditions in the experiments and simulations were limited to the case (f–f), free in both shell extremes, and case (c–f), clamped at the platform and free at the impact mass. In Fig. 5(a) the B250 shell was loaded quasi-statically in a press, while Fig. 5(b) shows the shape of a shell B250 clamped in the base using the fixture shown in Fig. 3, after being loaded with an impact kinetic energy of 757.8J ($G = 22$kg and $V_0 = 8.3$m/s). Figures 5(c), 5(d) and 5(e) are the final profile of the A shells after loaded with impact kinetic energies of 757.8J, 1505.8J and 8076.5J, respectively. Figures 6(a), (b) e (c) show C250 (f–f), C250 (c–f) and C500 (c–f) specimens loaded quasi-statically, while Fig. 6(d) is the result of C500(c–f) after being loaded with an impact kinetic energy of 1505.8J.

Figure 5: (a) B250 specimen loaded quasi-statically. (b)-(c) Clamped–free B250 and A250 specimens, respectively, loaded with $G = 22$kg and $V_0 = 8.3$m/s. (d)-(e) Free–free and clamped–free A500 specimen loaded with $G = 22$kg and $G = 118$kg, respectively, and $V_0 = 11.7$m/s.

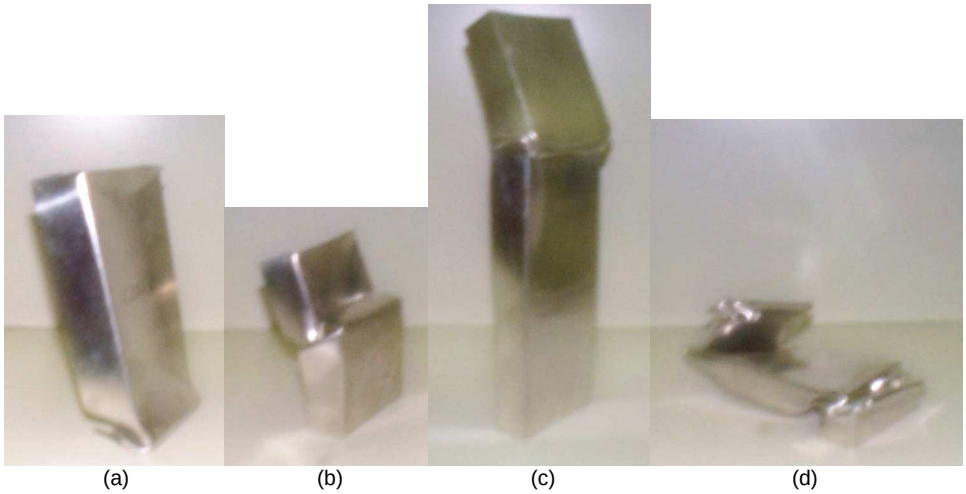

Figure 6: (a) C250 (f–f); (b) C250 (c–f); (c) C500 (c–f); (d) C500 (c–f). All them were subjected to $G = 22$kg and $V_0 = 11.7$m/s.

In order to explore the length influence in the colapse mode, some B specimens were manufactured with lenghts in the range of $L = 250$mm and $L = 500$mm. A mass $G = 31$kg travelling with a speed $V_0 = 12.2$m/s loaded the B (c–f) shells, Fig. 7. An approximate value of $L = 347$mm was found as the length transition between global and progressive buckling. These few experimental observations were used to calibrate the finite element model, as described below.

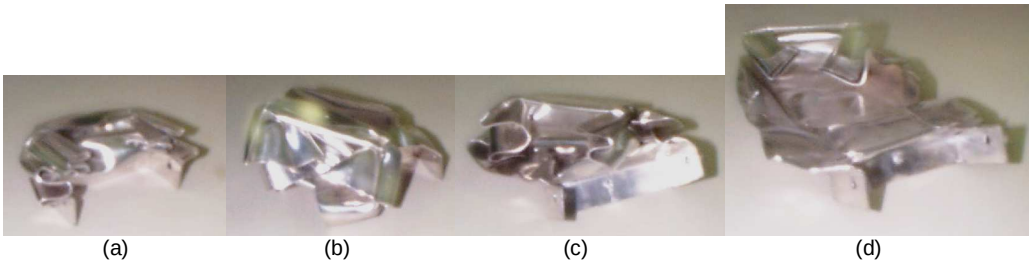

Figure 7: (a) B300 (c–f); (b) B338 (c–f); (c) B347 (c–f); (d) B400 (c–f). All them were subjected to $G = 31$kg and $V_0 = 12.2$m/s.

3. Finite-element modelling

Aiming at a better understanding of the buckling process, the open cross-section profiles were modelled using a general-purpose shell element type S4R available in ABAQUS. The three geometries used in the experiments were modelled using 5×5mm square shell finite elements. Mass elements were attached to the nodes of rigid

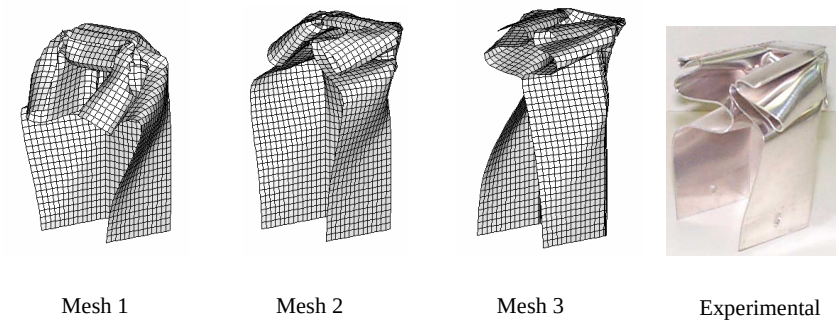

Figure 8: Studied FE models compared to the experimental result (for right) of a A250 specimen loaded by a mass of 22 kg at 8.3 m/s: Mesh 1 - Initial mesh ; Mesh 2 - mesh with geometric imperfections ; Mesh 3 - mesh obtained bending the laterals.

elements to give the total impact mass, and gravity was taken into account. Contact between surfaces was based on the concept of slave and rigid master surfaces. Two surface interactions were used, one between the stationary end of the specimen (slave) and the anvil (master) and another between the impacted end (slave) and the impact mass (master). In the explicit version used, self contact is automatically considered.

The initial Mesh 1 in Fig. 8 show a relatively poor correlation with the corresponding clamped–free experimental result in the same figure. Thus, imperfections along the shell length were added to the Mesh 1, following reference Karagiozova and Alves (2002) , where different amplitudes were attributed to the buckling modes. The numerical result for an impacted square tube in Jensen *et al.* (2001) was reproduced when attributing amplitudes of $(L/3000)$mm and $(L/60000)$mm to the first and third buckling modes, respectively. These same imperfections were used for the open shells, with the result illustrated in Fig. 8, Mesh 2.

Rigorously speaking, the actual specimens are not stress free due to the manufacturing process and highly localized strains are expected at the corners. Accordingly, a static finite element analysis was performed such that the blank aluminium sheet was bent and an open shell formed. This deformed mesh was subsequently subjected to axial impact and the results is shown in Mesh 3 of Fig. 8.

Since the deformed Meshes 2 and 3 in Fig. 8 are similar, despite of the complex analysis necessary to generate Mesh 3 due to the manufacturing simulation, it was decided not to model this effect in order to save computational time. It is also important to underline that it was observed, numerically, that a geometric variation of just one degree in the bending corners was sufficient to significantly affect the final buckling shape. This indicates that care must be exercised in modelling the buckled specimen. Fortunately, experimental buckled shapes were available and helped in choosing the very small imperfections adopted in the model.

All the results reported here for case (c–f) were simulated with no friction between the surfaces. A friction coefficient of 0.2 was used for the surfaces interaction in case (f–f), such that a good agreement between experiments and the numerical model was obtained based on the final collapse shape.

4. Numerical results and discussion

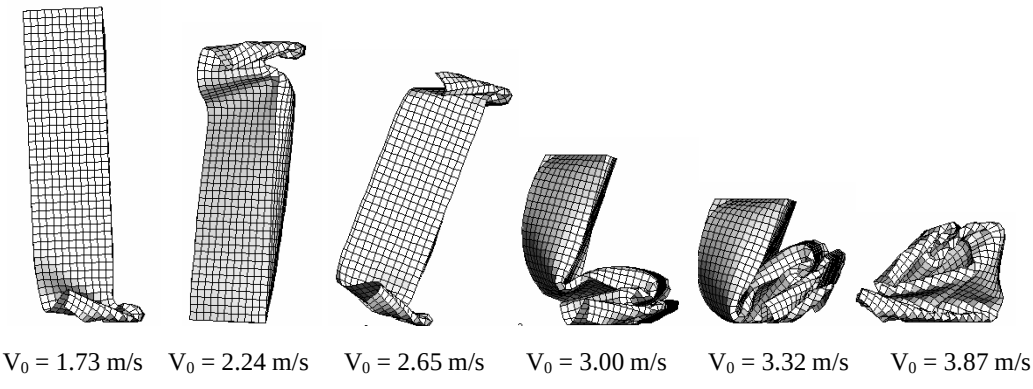

Figure 9: Free–free B250 specimen subjected to $G = 200$kg and impact velocities as indicated.

The A shells are inherently more stable than the B and C shells. No visual transition between progressive and global buckling for the A shell was detected in the many runs made with different impact velocities and

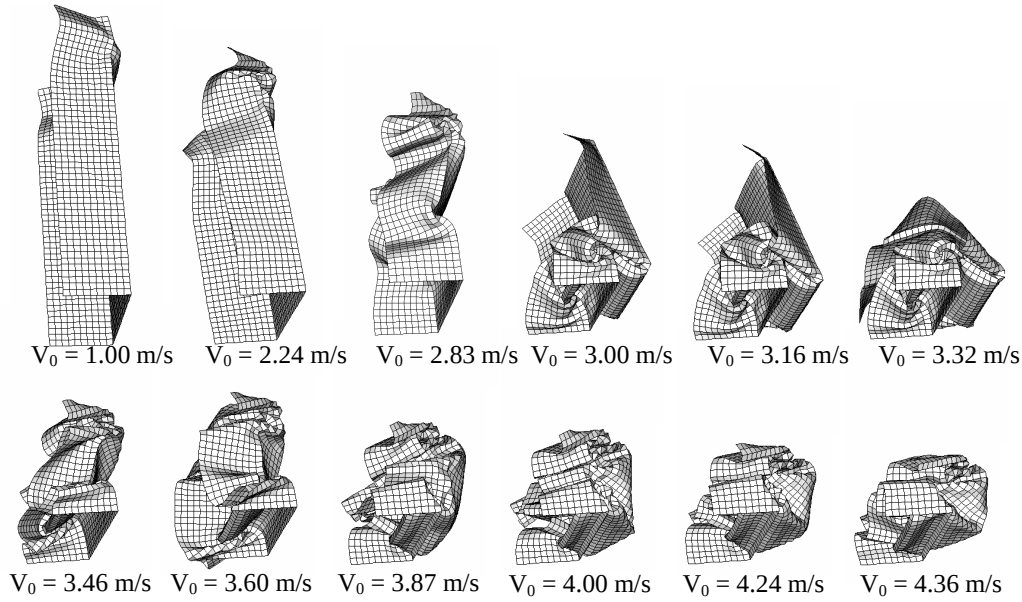

Figure 10: Same as in Fig. 9, but clamped–free.

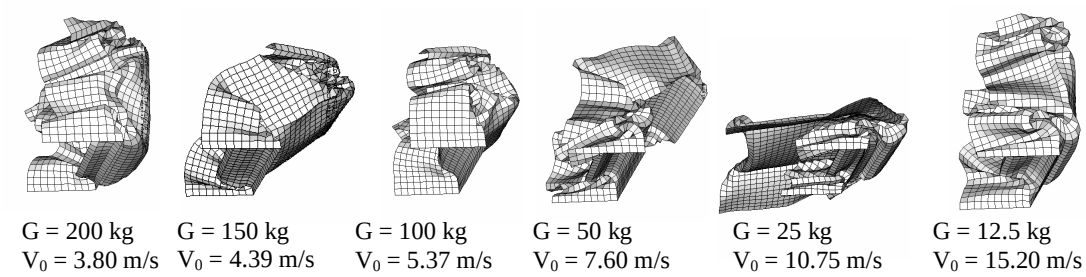

Figure 11: Clamped–free B250 shell tested with same initial energy of 1444J.

masses, even for $L = 500$mm. On the contrary, the B shells did present some features of the transition phenomenon, as it can be seen in Figs. 9 and 10 for the (f–f) and (c–f) cases, respectively. Obviously, the (c–f) B shells are more stable than the (f–f) case, as seen by comparing, for instance, the 3 m/s impact velocities cases.

The (f–f) B profile in Fig. 5(a), obtained in a press, indicates a clear global buckling, properly simulated when adopting $G = 1$E7kg and $V_0 = 18$E-3m/s. For higher impact velocities, Fig. 9, it was possible to notice that an increase of the impact velocity leads to a collapse mode closer to progressive buckling. A similar transition, from a more unstable to progressive collapse, occurred for the (c–f) B shells in Fig. 10.

However, fixing the impact energy at 1444J, and varying the impact mass and velocity accordingly, it can be seen in Fig. 11 that there is no unique collapse transition for these (c–f) B specimens. Figure 11 indicates that, by decreasing the impact mass, and so increasing the impact velocity, it is possible to obtain an unexpected global buckling (case $G = 25$kg) even for the high impact velocity of $V_0 = 10.75$m/s. This is in line with the work in Karagiozova *et al.* (2000), for cylindrical shells, whose authors found an important inertia effect for cylindrical shells.

It is interesting to observe from Karagiozaova and Alves (2002), that a small increase in the impact velocity alters the cylindrical shell response in Fig. 12 from a global to a progressive buckling collapse mode. The same reference also describes a phenomenon called inverse response, where an increase of the impact velocity from a progressive buckling stage, within some range, causes the shell to return to an unexpected global buckling response. Whether this is the case in Fig. 11 (see case $G = 25$kg) is difficult to say because the overall buckling shape of the specimens here studied do not lend an easy definition of the collapse mode, as in the case for the cylindrical shells presented in Fig. 12.

Intuitively, open sections are less stable than a closed shell. Even so, the lateral movement for the open shells is greatly facilitated, so permiting it to begin crushing in a progressive buckling mode. This can explain the difficulty of obtaining a clearer global mode of buckling and, hence, the transition.

Ideally, the load behaviour occurring during the folding process should be constant, which is rather difficult to occur and a peak load always takes place. Both values of the peak load, P_{max}, and the mean load

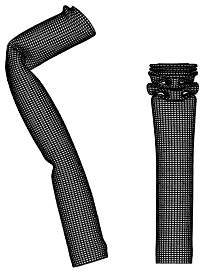

(a) (b)

Figure 12: Collapse shapes for circular aluminium shells with $L = 450$mm: (a)$V_0 = 6.0$m/s, (b)$V_0 = 6.25$m/s. [transition impact velocities](Karagiozova and Alves, 2002).

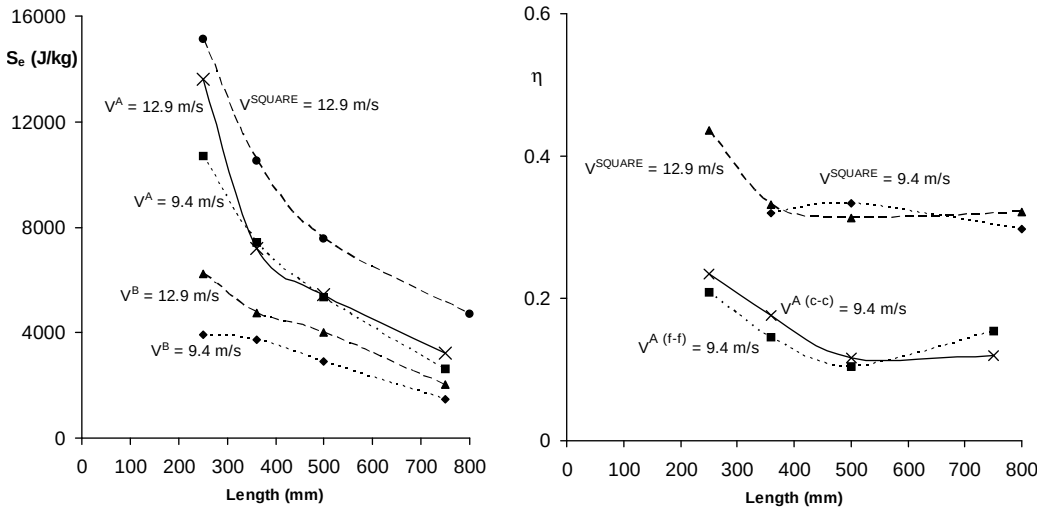

(a) (b)

Figure 13: Comparison of A, B and square (68×68mm) shells: (a) Specific energy; (b) Structural efficiency. Superscript to the impact velocity indicates specimen type and boundary conditions.

$$P_m = \frac{E_{ab}}{\delta_f}, \tag{1}$$

are an indication of the performance of the structure, where E_{ab} is the total absorbed energy and δ_f is the final axial displacement.

Experimental and numerical evidences here presented show that it is not obvious to apply the concepts of global and progressive collapse mode to these open profiles based only on the final deformed configuration. Hence, by defining the specific energy

$$S_e = \frac{E_{ab}}{m}, \tag{2}$$

where m is the mass of the specimen, one is more likely to draw some conclusions on the efficiency of the open profiles. Small (large) values of S_e would indicate a tendency to a global (progressive) buckling mode.

Accordingly, the curves in Fig. 13(a) were obtained from the FE analysis for cases (f-f) and $G = 50$kg. It is also presented results for the specific energy of a 68mm×68mm square tube. It can be noted that for a test under the same initial conditions the B profile, being slender, absorbs less energy than the A shell.

Notice that S_e in Fig. 13(a) increases with the impact velocity for both A and B profiles, indicating a more stable response. The opposite is true when the shell length is considered. S_e decreases for longer shells, suggesting a less progressive buckling mode. This remark stresses the importance of the impact velocity on the phenomenon here studied.

The structural effectiveness (η), defined as the mean axial crushing force divided by the product of cross–sectional area and yield stress,

$$\eta = \frac{P_m}{A\sigma_y}, \tag{3}$$

is plotted against the shell length in Fig. 13(b). The A shell is the same as the square shell except for the lack of one side. The results for (c–f) and (f–f) A specimen show that the boundary condition has an influence on the structural effectiveness of up to 20%, and that a square tube has a η of up to 287% larger than the A shell. For the range of V_0 showed, the square tube analysed always underwent progressive buckling, explaining the nearly constant structural effectiveness value.

5. Conclusions

The present investigation analysed some important parameters affecting the collapse mode of open shells. The impact velocity, impact mass, length and cross-section of shells were varied in order to assist in the future development of a buckling transition criterion. Numerical and experimental results lead to the conclusion that buckling transition from a global to a progressive mode cannot be clearly characterised for these open shells by considering only the overall final bucking shape, as it is the case for cylindrical shells. It was found that it seems more meaningful to use the specific energy to infer whether an impact response is more or less stable, so giving a more clear indicative of the collapse mode.

6. Acknowledgement

The support of FAPESP, grant 01/11300-8, is acknowledged.

7. References

Abramowicz, W. and Jones, N., 1986, "Dynamic progressive buckling of circular and square tubes", Inter. J. of Impact Eng., 4, pp. 243–270.

Abramowicz, W. and Jones, N., 1997, "Transition from initial global bending to progressive buckling of tubes loaded statically and dynamically", Inter. J. of Impact Eng., 19(5-6), pp. 415–437.

Alexander, J., 1969, "An approximate analysis of the collapse of thin cylindrical shells under axial load", Q. J. of Mechanics and Applied Mathematics, 13, pp. 10–15.

Alghamdi, A., 2001, "Collapsible impact energy absorbers: an overview", Thin-Walled Structures, 39, pp. 189–213.

Alves, M. and Birch, R., 1999, "Design of a structural impact rig", In "Brazilian Congress of Mechanical Engineering, Águas de Lindóia, SP".

Alves, M. and Jones, N., 2002, "Impact failure of beams using damage mechanics: Part II – application", International Journal of Impact Engineering, 27, pp. 863–890.

Alves, M. and Karagiozova, D., 2001, "Influence of the axial impact velocity on the buckling behaviour of circular cylindrical shells", In "9th National Conference on Theoretical and Applied Mechanics, Varna, Bulgária".

Alves, M. and Karagiozova, D., 2002, "Dynamic global and progressive buckling of circular shells under impact loads", In Khan, A. and Pamies, O. L., editors, "Plasticity, Damage and Fracture at Macro, Micro and Nano Scales", pp. 621–623.

Alves, M., Micheli, G. B., and Karagiozova, D., 2001, "Some experimental findings on the plastic buckling of shells under axial impact loads", In "Brazilian Congress of Mechanical Engineering, Uberlândia, MG".

Andrews, K., England, G., and Ghani, E., 1983, "Classification of the axial collapse of circular tubes under quasi-static loading", Inter. J. of Mechanical Sci., 25, pp. 687–696.

Chen, W. and Wierzbicki, T., 2001, "Relative merits of single cell, multi-cell and foam-filled thin-walled structures in energy absorption", Thin-Walled Struct., 39, pp. 287–306.

Guillow, S., Lu, G., and Grzebieta, R., 2001, "Quasi-static axial compression of thin-walled circular aluminium tubes", Inter. J. of Mechanical Sci., 43, pp. 2103–2123.

Hsu, S. S. and Jones, N., 2001, "Quasi-static and dynamic axial crushing of circular and square stainless steel tubes", In Jones, N., Brebbia, C. A., and Rajendran, A. M., editors, "Structures Under Shock and Impact VII", pp. 169–178. W.I.T.Press.

Jensen, O., Langseth, M., and Hopperstand, O. S., 2001, "Transition between progressive and global buckling of aluminium extrusions", In Jones, N., Brebbia, C. A., and Rajendran, A. M., editors, "Structures Under Shock and Impact VII", pp. 269–277. W.I.T. Press.

Karagiozova, D. and Alves, M., 2002, "Transition from progressive buckling to global bending of circular shells under impact", in preparation.

Karagiozova, D., Alves, M., and Jones, N., 2000, "Inertia effects in axisymmetrically deformed cylindrical shells under axial impact", Inter. J. of Impact Eng., 24, pp. 1083–1115.

Lu, G. and Mao, R., 2001, "A study of the plastic buckling of axially compressed cylin. shells with a thick-shell theory", Inter. J. of Mechanical Sci., 43, pp. 2319–2330.

Mahmood, H. F. and Paluszny, A., 1982, "Stability of plate-type box columns under crush loading", In "Computational Methods in Ground Transportation Vehicles", pp. 17–33.

White, M. D. and Jones, N., 1999, "Experimental study into the energy absorbing characteristics of top-hat and double-hat sections", Proceedings Institution of Mechanical Engineers, 213, pp. 259–278.

White, M. D., Jones, N., and Abramowicz, W., 1999, "A theoretical analysis for the quasi-static axial crushing of top-hat and double-hat thin-walled sections", Inter. J. of Mechanical Sci., 41, pp. 209–233.

Wierzbicki, T. and Abramowicz, W., 1983, "On the crushing mechanics of thin-walled structures", Journal of Applied Mechanics, 50, pp. 727–734.